Interaction of Ovalbumin with Phospholipids Langmuir−Blodgett Film

Tapanendu Kamilya, Prabir Pal, and G. B. Talapatra*

Department of Spectroscopy, Indian Association for the Cultivation of Science, Jadavpur, Kolkata-700 032, India

Received: June 1, 2006; In Final Form: December 11, 2006

Interaction of native ovalbumin (OVA) with 1,2-dipalmitoyl-*sn*-glycero-3-phosphocholine (DPPC) Langmuir−Blodgett monolayer has been studied at the air−water interface. A compressibility study shows the positive association with DPPC. Adsorption kinetics shows that the protein adsorption is a one-step process and the amount of protein adsorbed depends on the concentration of protein at the water subphase. Incorporation of protein into the DPPC layer is surface-pressure dependent. The compressibility study indicates that the DPPC−OVA interaction is hydrophobic in nature and structural reorganization is eminent to adjust the hydrophobic mismatch between DPPC acyl chains and OVA hydrophobic moieties. At higher pressure, OVA tends to squeeze out from the DPPC monolayer. A nanometer scale FE-SEM image confirms this observation. Globular aggregates of protein of dimension 60−80 nm were observed in DPPC−OVA supported film. Steady-state fluorescence spectroscopy suggests that the tryptophan residues of OVA are main emitting species. The blue shift of tryptophan fluorescence in supported film may be due to the tryptophan molecule of protein exposed to the hydrophobic air phase.

Introduction

Phospholipids and proteins are the main structural elements of cell membrane. Natural surfactant systems[1] in lungs, eyes, and ears are also made of equimolar amounts of saturated and unsaturated phospholipids and specific proteins.[2,3] , These properties have attracted considerable interest in the detailed study of phospholipids and proteins. Various techniques have also been introduced to immobilize biomaterials on solid matrix surfaces, such as self-assembly,[4] sol−gel process,[5] Langmuir−Blodgett (LB) techniques,[6] etc. Out of the various techniques, the Langmuir−Blodgett (LB) film deposition technique is a very useful tool in controlling the formation of ultrathin film. In addition, various works have been done to create the interfacial films of phospholipids and to study the surface morphology of phospholipids monolayer and bilayer as well as the incorporation of protein on various lipid surfaces.[7,8] Immobilization of protein without denaturation on a solid support has been found extremely valuable for chromatographic purification of a variety of drugs, peptides, proteins, and antibodies and for sensor application.[9,10]

Ovalbumin (OVA) is the major egg-white protein. It is a phosphorylated and glycosylated globular protein of 385 amino acids having molecular weight 45 kDa, soluble in water.[11] OVA contains three tryptophan residues; Trp_{148} in helix F, Trp_{267} in helix H, and Trp_{184} as the nearest neighbor residue of the carboxyl terminus of strand 3A.[12−14] OVA is a protein that has surface active property. OVA adsorbs at the air−water interface by exposing its hydrophobic moieties to the interface.[15,16] This adsorption starts with diffusion of protein from the bulk to interface. Near to the interface, protein goes from the dissolved to the adsorbed state. It was reported that protein concentration between 0.01 mg/mL to 3 mg/mL, OVA does not form foam.[15] Depending on molecular properties of OVA, the poor foaming behavior is responsible for its slow adsorption kinetics at air−water interface.

In this paper, the interaction of a soluble surface-active protein OVA with an insoluble monolayer of 1,2-dipalmitoyl-*sn*-glycero-3-phosphocholine (DPPC) was studied. By combined use of LB deposition and FE-SEM techniques, this study focused on the structural organization of OVA on the DPPC monolayer. Here the lipid−protein interaction was studied by measuring the surface pressure (π) versus time (t) and the surface pressure (π) versus area (A) isotherms. Moreover, the surface morphology of DPPC film, OVA film, and OVA-DPPC mixed films were successfully studied by FE-SEM. Steady-state fluorescence spectroscopy was used to study the tryptophan fluorescence of protein. The effect of surface pressure on film morphology has also been studied.

Experimental Section

1,2-Dipalmitoyl-*sn*-glycero-3-phosphocholine and ovalbumin were purchased from Sigma Chemical Co. These chemicals were used as received without further purification. Spectral grade chloroform (SRL, India) was used to prepare solutions of DPPC with the desired concentration. The subphase was triple distilled water, deionized with a Milli-Q water purification system from Millipore. The pH and resistivity of the distilled water were 6.8 and 18.2 MΩ cm respectively. Teflon-bar-barrier type LB trough (model 2000C, Apex Instruments Co., India) was used for monolayer film preparation, characterization, and deposition. All experiments were performed at 26 ± 1°C unless otherwise mentioned.

For preparation of pure OVA monolayer, a known amount of an aqueous solution of OVA of concentration of 0.01 mg/mL was spread on the water subphase by a microsyringe. After waiting for 20 min, the monolayer was slowly compressed with a compression speed of 1 Å^2/(molecule·min).

For the preparation of the pure DPPC monolayer, a chloroform solution of DPPC (1 mM) was spread on the water

* To whom correspondence should be addressed. E-mail: spgbt@iacs.res.in.

10.1021/jp063377l CCC: $37.00
Published on Web 01/19/2007

subphase. After a delay of 20 min to allow the solvent to evaporate, the monolayer was slowly compressed to the desired pressures with a compression speed of 1 Å^2/(molecule·min). Finally, after 2 h of stabilization, the monolayer was transferred very carefully with a speed of 5 mm/min onto hydrophilic quartz slides and glass cover slips, which were previously immersed in the subphase. The glass substrates were cleaned in a liquid soap ultrasonic bath followed by repeated rinsing with Millipore water before use. They were then immersed in acetone in an ultrasonic bath. Finally, they were cleaned using Millipore water in the ultrasonic bath. A uniform layer of water onto the slide confirmed the hydrophilicity of the slide.

For the preparation of OVA-DPPC LB films, first we mixed OVA in the subphase with various concentrations of protein, C_{OVA} (0.0001, 0.001, 0.01 mg/mL), and then DPPC solution was spread on this protein-containing subphase. Finally, the films were transferred using the process as stated previously.

To study the adsorption kinetics of OVA in the DPPC monolayer, at first, the pure DPPC monolayer was precompressed to requisite pressure and then OVA was injected into the subphase to attain the required final concentration.

Cast films were prepared on clean hydrophilic quartz or glass substrate by evaporation technique. A drop of aqueous solution (0.001 mg/mL) of protein was placed on the slide and was kept in a desiccator with nitrogen atmosphere for the evaporation of solvent.

A hydrophilic quartz slide was dipped into 0.01 mg/mL of OVA solution for 6 h. The slide was then lifted from the OVA solution and very carefully rinsed with Millipore water and dried. Then the fluorescence spectra of protein were monitored. That no detectable fluorescence was observed ensured that there was no adsorption of OVA onto the immersed slide.

DPPC vesicles were prepared by the ethanol injection method.[17,18] A solution of 20 mg of DPPC dissolved in 500 μL of ethanol was rapidly injected, using a microliter syringe, into 20 mL of deionized water at 45 °C. This method produces a heterogeneous population of vesicles with diameters ranging from a few micrometers to 100 nm. After injection, the mixture was kept for 1 h at 45 °C, that is, above the gel transition temperature (41.5 °C) of DPPC.[17,18] A quantity of 0.1 mg/mL of protein solution was preheated to 45 °C. This solution (1 mL) was then added to a 45 °C preheated 3 mL DPPC vesicle solution (DPPC/OVA was 30:1 by weight) and kept at 45 °C for 1 h. Fluorescence spectra of this solution were measured at 45 °C. The whole solution of vesicles with protein was cooled to 26 °C to measure the fluorescence below the transition temperature.

Fluorescence spectra of the OVA solution, OVA cast film, and DPPC−OVA films on quartz slides were measured with a Hitachi F-4500 spectrometer. The surface morphology of all the films was studied by high-resolution field emission scanning electron microscope (FE-SEM, model no. JEOL JSM-6700 F).

Results and Discussion

A. π−A Isotherm. Surface pressure (π)−area (A) compression isotherms of LB monolayer of pure OVA, pure DPPC, and DPPC−OVA with various concentrations (0.0001, 0.001, 0.01 mg/mL) of OVA in water subphase were collected.

π−A Isotherm of Pure OVA. Figure 1 represents the typical π−A isotherm of pure OVA. When the area/molecule is about 4.7 nm^2/OVA, the surface pressure begins to rise. The OVA molecule has an ellipsoidal shape with dimensions of 7 nm × 4.5 nm × 5 nm (PDB 1OVA).[19] Therefore, the estimated calculated value of area/molecule should be in the range of 25−35 nm^2/OVA, depending on the orientation. The observed area/molecule from the π−A isotherm is much less than the calculated value. This indicates that some OVA molecules may dissolve into the subphase. It is known that the protein cannot dissolve into the water subphase with high salt (KCl) concentration (∼ 3.5 M).[20] In that case, one should get true area/molecule. We do not use salt solution for the OVA isotherm measurement as salt solution may perturb the OVA isotherm.[20] π−A isotherm of OVA contains gaseous (G), liquid (L), and collapse of monolayer. Several features are clearly seen in the isotherm: (a) in a region from area/molecule 4.7 to 3.03 nm^2, surface pressure rises very slowly from 0 to ∼1.45 mN/m. In this surface pressure region, a large decrease in molecular area is observed with a slight increase in surface pressure. This behavior may be due to G to L transition. (b) Afterward, there is a monotonous increase of pressure up to 25 mN/m. In this region, the monolayer is in L state. (c) After that, a plateau is observed between the surface pressures from 25 to 35 mN/m. The origin of this plateau at the higher surface pressure is not very clear. However, this may be due to some type of phase change like liquid-expanded (LE) to liquid-condensed (LC) as explains the case of apolipoproteins (APO)[20−22] or may be due to partial squeeze-out of the protein (or part of the protein) preceding the full collapse. The FE-SEM images of films transferred at 35 mN/m presented in Figure 9 supports the latter. Details of discussion of FE-SEM images are discussed later. The origin of squeeze-out of the protein is not very clear to us, but the desorption of hydrophobic moieties of OVA from the air−water interface due to high pressure may be the cause of squeezing out of protein.

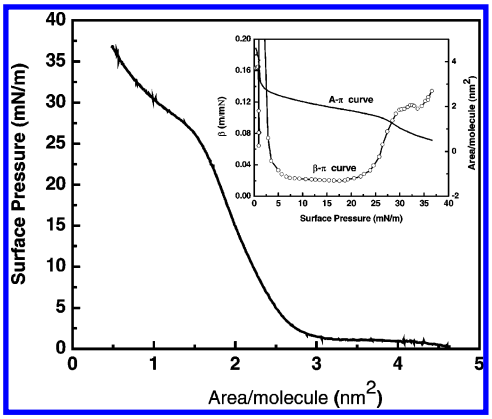

Figure 1. Plot of pressure−area isotherm at room temperature (26 °C) of pure OVA. Inset figure represents the $\beta-\pi$ plot (left-hand scale) and A−π plot (right-hand scale) for pure OVA.

π−A Isotherm of Pure DPPC and DPPC−OVA Mixed Monolayer. Figure 2 shows the π−A isotherm of pure DPPC and the DPPC−OVA mixed monolayer. The isotherm of the pure DPPC LB monolayer is well-known. It is shown here mainly to compare it with the isotherms of the DPPC−OVA complex monolayer. π−A isotherm of pure DPPC shows a plateau like region. This plateau originates because of phase coexistence, associating with the first-order phase transition between the liquid-expanded (LE) and liquid-condensed (LC) states.[23,24] This is a process of aggregation of molecules.

The π−A isotherms of the OVA mixed DPPC monolayer show that with increasing concentration of OVA in the water subphase, the area/molecule of DPPC increases. Probably two processes, one related to the transport/diffusion of OVA at the surface and the other the interaction of OVA with DPPC molecules at the surface, control this observation. An additional hump appears at higher pressure and becomes more prominent

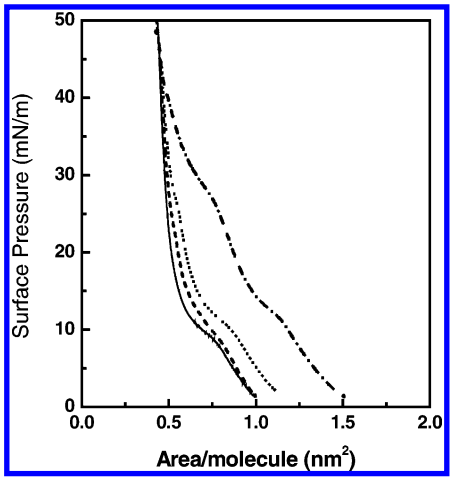

Figure 2. Plot of pressure−area isotherms at room temperature (26 °C) of DPPC with different concentration of OVA in water subphase: (—) pure DPPC, (---) 0.0001 mg/mL, (•••) 0.001 mg/mL, and (-•-•-•-) 0.01 mg/mL.

with increasing protein concentration. Compared with the isotherm (Figure 1) of pure OVA, this hump may easily be identified as an L to collapse transition of protein associated with a partial squeeze-out of the protein (or a part of the protein). From Figure 2, it is distinct that in the condensed region (at surface pressure ∼ 43 mN/m) all the π−A isotherms of the DPPC−OVA mixed monolayer tend to overlap with the isotherm of pure DPPC. This may indicate successive squeezing-out of protein at high surface pressure.[25,26]

B. Compressibility Study. For better characterization and explanation of phase transition, two-dimensional compressibility of the monolayer has been introduced. For the calculation of compressibility coefficient, the following equation was used.[27]

$$\beta = -(1/A) \times (\delta A/\delta \pi)_T \qquad (1)$$

It is very interesting that any phase-transition phenomenon may be represented by the $\beta-\pi$ curve in a better way. The peaks indicate the maximum compressibility (β_{max}) of the monolayer. The maximum compressibility indicates maximum intermolecular cooperativeness. The transition range is very clearly identified by the help of $\beta-\pi$ curve. The asymmetry of the peak indicates that phase transition may consist of several steps.[28]

$\beta-\pi$ curves of pure DPPC and DPPC−OVA with different OVA concentration (C_{OVA}) at 26 °C, together with original π−A curve for comparison, are illustrated in Figure 3. The inset of Figure 1 also shows the $\beta-\pi$ curve of pure OVA. For pure DPPC there is only one phase-transition region. The peak is asymmetric. Deconvolution of this asymmetric peak (shown in Figure 4) shows LE−LC phase transition for pure DPPC is two-step processes. It may be due to two types of molecular reorientation in the region of lipid head group. Results are quite similar to the result reported earlier.[28]

The $\beta-\pi$ curves for DPPC mixed OVA show two transition regions. The low-pressure phase transition represents the LE−LC phase transition in DPPC. Here peaks are also asymmetric (Figure 3), indicating multistep processes are involved. Compared with pure DPPC, the β_{max} of the first peak is apparently OVA concentration dependent. The value of β_{max} apparently decreases with increasing amount of incorporation of OVA in the DPPC monolayer. There is a shift of the peak toward higher pressure with increasing protein incorporation (Figure 5). The second peak at higher pressure appears in the presence of OVA. However, this is absent in pure DPPC. Here we see that maximal

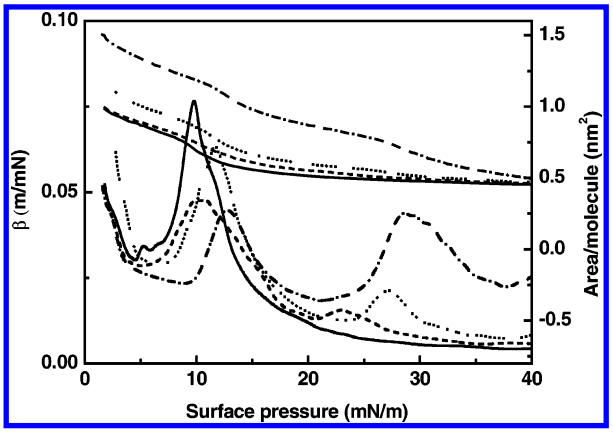

Figure 3. $\beta-\pi$ plot at room temperature (26 °C) for pure DPPC and DPPC−OVA mixed monolayer for different protein concentrations in water subphase: (—) pure DPPC, (---) 0.0001 mg/mL, (•••) 0.001 mg/mL, and (-•-•-•-) 0.01 mg/mL. The corresponding A−π plot (right-hand scale) is also shown for comparison.

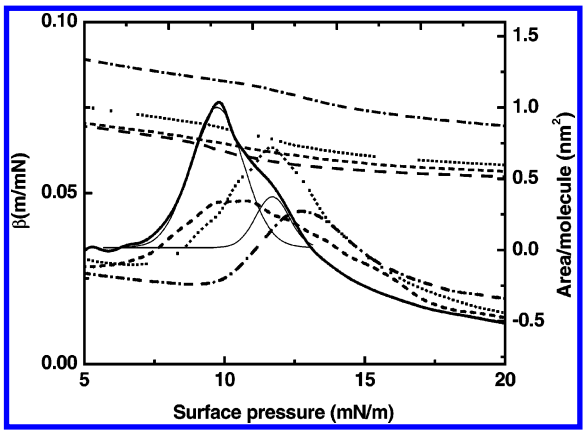

Figure 4. $\beta-\pi$ plot at room temperature (26 °C) for pure DPPC and DPPC OVA mixed monolayer in the first phase transition region: (—) pure DPPC, (---) 0.0001 mg/mL, (•••) 0.001 mg/mL, and (-•-•-•-) 0.01 mg/mL. $\beta-\pi$ curve for pure DPPC is deconvoluted into two peaks showing two distinct steps.

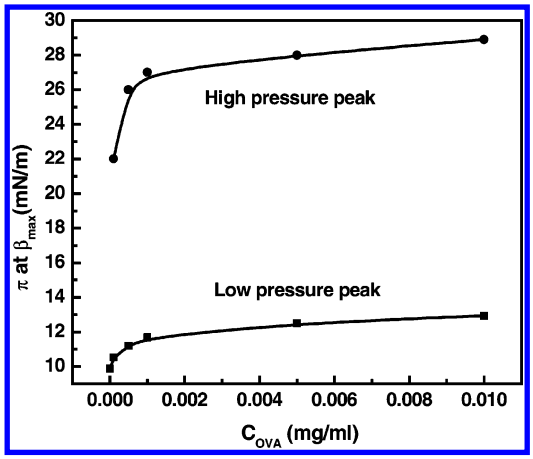

Figure 5. Protein concentration (C_{OVA}) versus surface pressure at β_{max}. The curve lines are a spline fit of experimental data.

compressibility increases, and a shift of this peak toward higher pressure occurs with increasing concentration of protein (Figure 5). The shift in the DPPC phase transition (LE−LC) region to higher pressure is probably due to the interaction of protein with DPPC. The exact nature of interaction is not so clear. DPPC has a distinct hydrophobic end (acyl chains); OVA also has distinct hydrophobic moieties. Thus, hydrophobic interaction is expected to play a major and important role in the process of

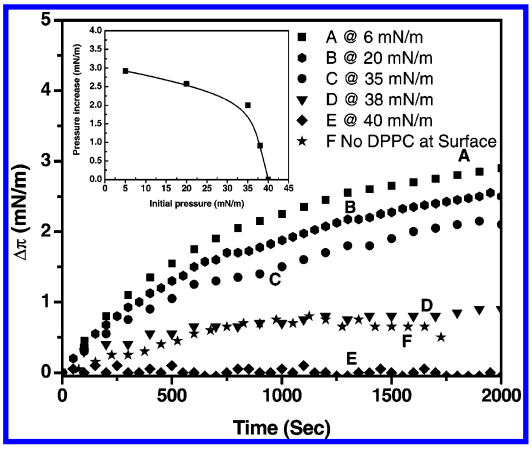

Figure 6. Change in surface pressure ($\Delta\pi$) with time for 0.01 mg/mL OVA in the water subphase at different precompressed DPPC monolayers indicated in the figure. Zero time is adjusted to the time when the rising of pressure starts. The inset shows change in pressure vs the initial pressure of the DPPC precompressed monolayer in the presence of 0.01 mg/mL OVA in water subphase at 2000 s. The line is a B-spline fit.

incorporation of OVA into the DPPC monolayer at the interface.[29] When an OVA molecule approaches the DPPC monolayer, the hydrophobic part goes into the interface. There may be a hydrophobic mismatch between DPPC and OVA. To minimize the mismatch, the configuration of the DPPC acyl chains may be altered, which subsequently affects the LE−LC phase change region of DPPC to shift the phase transition at higher pressure. A similar explanation may be made for the second-transition region of OVA also. However, the structural modification of the protein makes it also possible to minimize the hydrophobic mismatch, which subsequently leads to a shift in peak to lower pressure.[29−32]

C. Adsorption Kinetics. We have studied adsorption kinetics of pure OVA and OVA with a DPPC monolayer at the air−water interface. Figure 6, tracesA−E represent the time dependent change in surface pressure of the DPPC monolayer precompressed at various surface pressures when a fixed amount (0.01 mg/mL final concentration) of protein was injected beneath the DPPC monolayer in the water subphase. It is found that the change in pressure for the precompressed DPPC monolayer in the condensed region is less compared to that of in the LE region. A progressively lower increase in pressure upon the interaction of the OVA with the lipid films compressed to higher initial pressure occurs. At a pressure of ∼38 mN/m, a very small amount of protein uptake occurs, whereas at 40mN/m, no further increase in pressure was observed. The inset of Figure 6 shows the plot of the initial pressure versus the change in pressure at a particular protein concentration (0.01 mg/mL) in the subphase water. This plot gives the value of critical pressure: $\pi_c \approx 40$ mN/m. Critical surface pressure is the pressure at which protein cannot produce any further increase of surface pressure. Similar observations were made for puroindoline in the DPPC and in the DPPG monolayer.[33] Generally, this type of plot follows a linear dependence.[33] However, in our experiment, the nature of the plot is curve. A probable explanation is that here the concentration of protein used was very low, and we have measured pressure up to 2000 s, which may not be a sufficient time to reach the equilibrium. The overall results indicate that the incorporation of protein is more favorable at the LE region.

Figure 6F shows the result of surface activity of the OVA. This figure shows the increase of surface pressure for 0.01 mg/mL of protein solution in pure water (pH 6.8) when no DPPC is present. This change is less in the presence of the DPPC

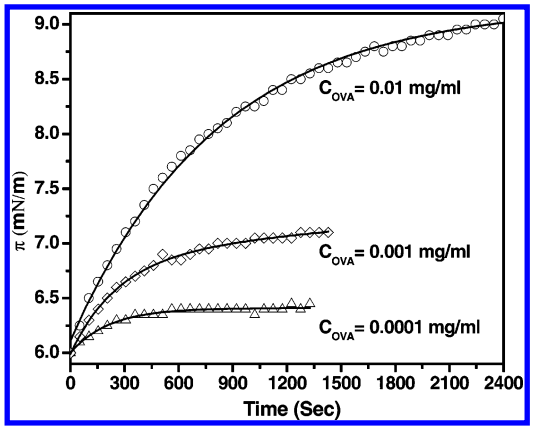

Figure 7. Adsorption kinetics of OVA with different concentrations of OVA in water subphase. Curved lines are the fitting curves using eq 2. Zero time is adjusted to the time when the rising of pressure starts.

TABLE 1: Fitting Parameters Using Equation 2 of Adsorption Kinetics of Ovalbumin with Different Ovalbumin Concentrations in Water Subphase[a]

protein concn (mg/mL)	k (s^{-1})	a (mN/m)	c (mN/m)	R^2
0.0001	$4.64 \times 10^{-3} \pm 7.9\%$	$6.00 \pm 0.26\%$	$6.41 \pm 0.09\%$	0.97
0.001	$2.78 \times 10^{-3} \pm 3.9\%$	$6.02 \pm 0.28\%$	$7.10 \pm 0.15\%$	0.99
0.01	$1.23 \times 10^{-3} \pm 0.81\%$	$6.11 \pm 0.26\%$	$9.17 \pm 0.06\%$	0.99

[a] The values a and c are the initial and final surface pressure of the monolayer and k is the apparent first-order rate constant. R is the residual correlation coefficient.

monolayer precompressed at low surface pressure (Figure 6A−C), and saturation is reached within 10−15 min. However, in the presence of the DPPC monolayer, more time is required to reach the saturation value. This clearly indicates the definite interaction of the OVA with the DPPC monolayer.

For analyzing the kinetics of incorporation of OVA into the DPPC monolayer in the LE region (6 mN/m), we have studied the change in pressure with time at different OVA concentration in water subphase. Figure 7 represents such plots.

To analyze the kinetics, the data of Figure 7 were fitted to a simple first-order reaction mechanism. In this case, we used the following equation[6]

$$\pi = c + (a - c)^* \exp(-kt) \qquad (2)$$

Where a, c, and k are fit parameters: a and c are the initial and final surface pressure of the monolayer and k is the apparent first-order rate constant. The results are shown in Figure 7 and the parameters resulting from the fits are summarized in Table 1. We have also tried sequential fitting[6] for the multistep process. The agreement of the experimental and the fitted curves shows that the kinetics of the penetration reaction is adequately described by a one-step first-order reaction. This represents that the incorporation of protein to the DPPC monolayer is a one-step process. From Table 1, one can see that the rate constant k, increases with protein concentration. It is found that value of k and c reaches a saturation value at a higher concentration (0.01 mg/mL). This indicates that the amount of incorporation of protein increases with increasing concentration and reaches a maximum at a higher concentration.

Surface activity of protein is due to the diffusion of proteins from the bulk to the interface. Close to the interface, protein can go from the dissolved to the adsorbed state. The main reason for this adsorption is the decrease of exposure of hydrophobic moieties to the aqueous medium.[34] The presence of DPPC at the air−water interface facilitates this diffusion of protein to

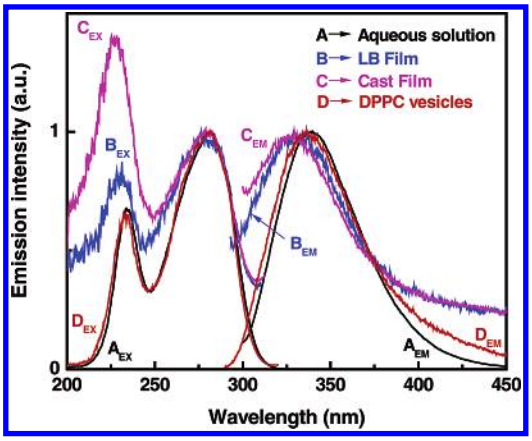

Figure 8. Peak normalized emission (λ_{ex} = 280 nm) and excitation (λ_{em} = 340 nm) spectra of OVA in different conditions: (A) 0.0001 mg/mL aqueous solution of OVA; (B) OVA-DPPC mixed LB monolayer lifted at 35 mN/m pressure; (C) cast film; and (D) DPPC vesicles with OVA. The suffixes EX and EM represent excitation and emission spectra, respectively.

the surface. In all experiments, the pH of the aqueous medium was kept at 6.8. In this pH, DPPC is known to be zwitterionic[35] and the net charge of OVA is −7.[36] Some induced electrostatic interaction together with hydrophobic interaction may be responsible for a higher accumulation of protein at the air−water interface in the presence of DPPC.

D. Steady-State Fluorescence Spectroscopy. OVA is known to have three tryptophan residues. These residues are responsible for fluorescence of the protein molecule. We have measured the fluorescence and excitation spectra of OVA in water solution, in cast film, and OVA bound in DPPC LB film. Normalized emission and excitation spectra are shown in Figure 8. Fluorescence spectra of OVA confirms that it consists of tryptophan because emission spectra are in the range of tryptophan fluorescence.[37] Fluorescence excitation spectrum (λ_{em} = 340 nm) of OVA gives two peaks, one at 280 nm (L-peak) and another at 230−235 nm (S-peak). The short wavelength band is known to ^1B_b transition while the long wavelength band consists of the two overlapping transitions ^1L_a and ^1L_b with vectors almost perpendicular to each other. ^1L_a transition is sensitive to polarity and is believed to the main contributor to the emission.[38] From aqueous solution to cast film, the intensity of the S-peak increases relative to the L-peak. This may indicate that there may be some structural modification of the OVA molecule because of cast film formation. The variations of the L-peak and S-peak intensities of tryptophan excitation owing to the environment were reported in the literature.[39] In OVA-DPPC mixed film, these variations are small. This may indicate a little perturbation of the OVA structure. There is not much change in the positions of the peaks in the excitation spectrum for the changing environment of OVA. In the emission spectrum, the emission peak is shifted from 340 to 330 nm from aqueous solution to thin film. Full width at half-maximum (fwhm) is also decreased from 56 to 46 nm. The emission spectrum of OVA in aqueous solution corresponds to the type-II[38] emission spectrum of tryptophan residue, which is closer to a polar water molecule. In thin film, water is absent so the emission spectrum corresponds to the type-I emission spectrum of tryptophan residue that is free from the water or polar group.[38] The blue shift of tryptophan fluorescence in the supported film may be due to the exposure of tryptophan residues to a more hydrophobic environment. This can happen by burying protein inside the acyl chains matrix of DPPC. To check this argument, we measured the emission and excitation spectra of OVA in DPPC vesicles below (26 °C) and above (45 °C) the gel transition temperature (41 °C). Above the gel transition temperature, no appreciable shift in emission peak relative to that in aqueous solution was observed. A blue shift around 2 nm is apparent which may be within the limit of experimental error (Figure 8). Below gel transition temperature, fluorescence quenching was observed without any peak shift (data not shown). It implies that in a vesicle, the tryptophan residue of OVA is still in an aqueous environment. A similar observation in the DPPC vesicle for pulmonary surfactant protein-A was reported.[40] It is known that if unfolding or a denaturation of protein occurs, the emission peak shifts toward red, and it should be observed at about 350−355 nm in aqueous medium.[37] Our feeling is that ∼10 nm blue shift in supported film is solely due to the absence of a polar aqueous environment and the presence of a hydrophobic air environment by which OVA molecules undergo a conformational change, affecting its aromatic residues. It is very difficult to make any conclusion about the nature of folding and unfolding of protein in supported film (without water) by monitoring the fluorescence peak shift of tryptophan. However, a hydrophobic denaturation due to the opening of protein molecules when exposed to the hydrophobic air phase may be expected to produce exposition of the tryptophan residues to the air with a blue shift in fluorescence. This kind of interfacial denaturation has been well documented for other proteins like Bovine serum albumin and Bovine plasma fibrinogen.[41] Therefore, OVA molecules undergo a conformational change, affecting their aromatic residues, when they are exposed to the air−water interface.

E. Surface Morphology of Transferred Monolayer. The surface morphology of all of the transferred LB monolayer has been studied by high-resolution FE-SEM. Figure 9A shows the surface morphology of the pure DPPC monolayer (35 mN/m) transferred on hydrophilic glass substrate. The FE-SEM image of bare glass (Figure 9F) with the same resolution is also shown as a reference for comparison. The DPPC is at the LE region; the film is not compact, and the formation of domain is just beginning to start (not shown in figure). At the condensed state (35 mN/m), the film is rigid with a distinct nanometer-scale domain formation (Figure 9A). In this compact film, domains are of the order of 20−30 nm with some holes in the order of a few nanometers to 100 nm. These domains may be aggregates of DPPC. With a further increase of pressure, no appreciable change is observed.

Figure 9B shows the surface morphology of OVA cast film. Cast film remarkably shows a uniform structure of nanometer-scale protein clusters. Dimensions are in the range of 20 to 50 nm. We said earlier that the OVA molecule has an ellipsoidal shape with dimensions of 7 nm × 4.5 nm × 5 nm including four free sulfhydryl groups and one internal disulfide bond (PDB 1OVA).[14,19,42] Therefore, in Figure 9B nanoclusters represent aggregates of a few protein molecules.

Figure 9, panels C and D show the surface morphology of the OVA-DPPC monolayer at the LE state (5 mN/m) and condensed state (35 mN/m), respectively. The LE state film shows smooth surface morphology and looks like protein mixed DPPC film. In the condensed region, the film morphology is quite different. The surface is rough and globular domains are peeping out of the surface. We believe that these are globular domains of protein. The sizes of these domains are in the range of 40−80 nm. Absence of these domains at low pressure indicates that at the condensed region proteins are squeezed out

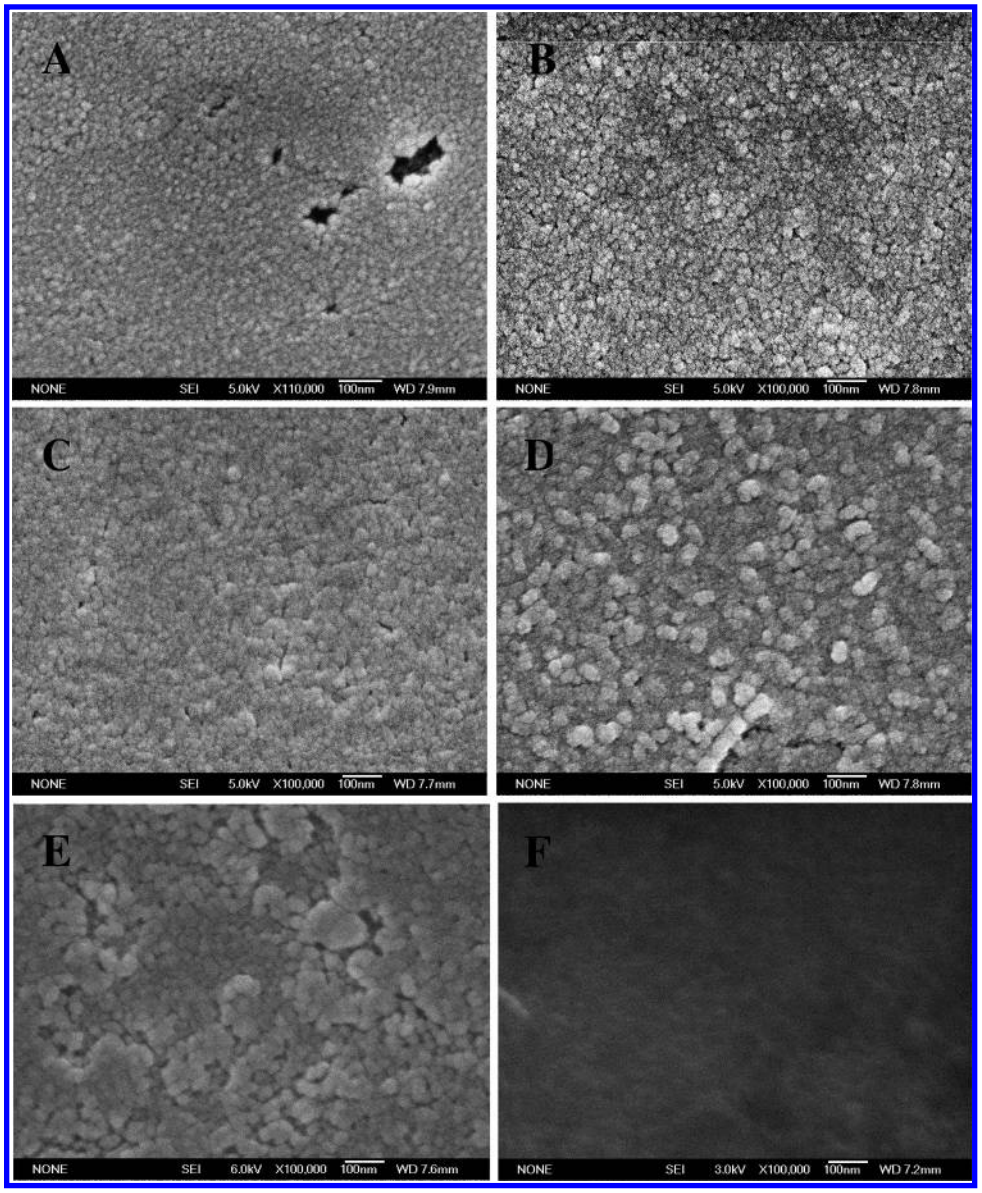

Figure 9. Nanometer scale resolution FE-SEM images: (A) DPPC single layer lifted at 35 mN/m pressure; (B) cast film of OVA; (C) DPPC−OVA (C_{OVA} = 0.0001 mg/mL) single layer lifted at 5 mN/m pressure; (D) DPPC−OVA (C_{OVA} = 0.0001 mg/mL) single layer lifted at 35 mN/m pressure; (E) DPPC−OVA (C_{OVA} = 0.001 mg/mL) single layer lifted at 35 mN/m; (F) bare glass slide.

from the DPPC monolayer and attached to the surface of the DPPC film. Compared with the OVA molecular dimension mentioned previously, one can say that these domains are aggregates of protein molecules. However, aggregates of protein capped with DPPC may not be ruled out. A similar domain structure of protein in a phospholipid membrane is observed by others.[27,43] With a higher concentration of protein, these protein clusters tend to amalgamate to form a layer of protein on the DPPC film (Figure 9E). A clear domain boundary in the protein layer indicates that OVA aggregates may cap with DPPC.

Conclusion

In this paper, we demonstrated the interaction of soluble OVA to the insoluble zwitterionic DPPC monolayer. Incorporation of protein into the DPPC monolayer is found to be surface pressure dependent and more in the LE region than in the condensed region. The critical pressure (π_c) at which protein does not penetrate the DPPC monolayer is found to be about 40 mN/m. Protein adsorption kinetics suggests that the adsorption process is one-step process. The compressibility study shows that there are two transition regions in the DPPC−OVA mixed monolayer. One is a LE to LC phase change of DPPC at the low-pressure region and the other is a L to collapse of OVA at the high-pressure region. The shifting of these transition regions with protein concentration indicates structural modification of protein as well as acyl chains of DPPC. A mismatch between hydrophobic moieties of protein and DPPC acyl chains and their subsequent adjustment is responsible for these shifts. At high pressure, protein is squeezing out of the DPPC monolayer. FE-SEM images also support this observation. Domains of protein-aggregates of size of 60−80 nm are observed at low protein uptake. At high protein uptake, these domains are amalgamated to the protein layer. The distinct domain boundary in the protein layer indicates the possibility of capping of the OVA by DPPC. Emission and excitation spectra of OVA indicate tryptophan residues are the main emitting species. In the supported film, a 10 nm blue shift of tryptophan fluorescence is solely due to the tryptophan molecule of protein being exposed to the hydrophobic air phase.

Acknowledgment. We thank DST, Government of India (Project No. IDP/Sen/94/03) for partial financial support. We also thank Mr. S. Maji for operating the FE-SEM.

References and Notes

(1) Serrano, A. G.; P'erez-Gil, J. *Chem. Phys. Lipids* **2006**, *141*, 105.
(2) Goerke, J. *Biochim. Biophys. Acta* **1998**, *1408*, 79.
(3) Pérez-Gil, J.; Keough, K. M. *Biochim. Biophys. Acta* **1998**, *1408*, 203.
(4) Kim, K.; Kim, C.; Byun, Y. *Langmuir* **2001**, *17*, 5066.
(5) Qu, H.; Wang, H.; Huang, Y.; Zhong, W.; Lu, H.; Kong, J.; Yang, P.; Liu, B. *Anal. Chem.* **2004**, *76*, 6426.
(6) Pal, P.; Nandi, D.; Misra, T. N. *Thin Solid Films* **1994**, *239*, 138.
(7) Wierenga, P. A.; Meinders, M. B. J.; Egmond, M. R.; Voragen, A. G. J.; de Jongh, H. H. J. *J. Phys. Chem. B* **2005**, *109*, 16946.
(8) Rosengarth, A.; Wintergalen, A.; Galla, H.; Hinz, H.; Gerke, V. *FEBS Lett.* **1998**, *438*, 279.
(9) Beigi, F.; Lundahl, P. *J. Chromatogr., A* **1999**, *852*, 313.
(10) Nguyen, T.; McNamara, K. P.; Rosenzweig, Z. *Anal. Chim. Acta* **1999**, *400*, 45.
(11) Nisbet, A. D; Saundry, R. H.; Moir, A. J. G.; Fothergill, J. E. *Eur. J. Biochem.* **1981**, *115*, 335.
(12) Wright, H. T.; Qian, H. X.; Huber, R. *J. Mol. Biol.* **1990**, *213*, 513.
(13) Stein, P. E.; Leslie, A. G.; Finch, J. T.; Turnell, W. G.; McLaughlin, P. J.; Carrell, R. W. *Nature* **1990**, *347*, 99.
(14) Stein, P. E.; Leslie, A. G.; Finch, J. T.; Carrell, R. W. *J. Mol. Biol.* **1991**, *221*, 941.
(15) Wierenga, P. A.; Meinders, M. B. J.; Egmond, M. R.; Voragen, F. A. G. J.; De, Jongh, H. H. J. *Langmuir* **2003**, *19*, 8964.
(16) Benjamins, J.; Lyklema, J.; Lucassen-Reynders, E. H. *Langmuir* **2006**, *22*, 6181.
(17) *Liposomes: A Practical Approach*; New, R. R. C., Ed.; Oxford University: Oxford, 1990; p 63.
(18) Stryer, L. *Biochemistry*; Freeman: New York, 1998; p 271.
(19) Protein Data Bank (PDB 1OVA).
(20) Xicohtencatl-Cortes, J.; Mas-Oliva, J.; Castillo, R. *J. Phys. Chem. B* **2004**, *108*, 7307.
(21) Bolanos-Gracia, V. M.; Mas-Oliva, J.; Ramos, S.; Castillo, R. *J. Phys. Chem. B* **1999**, *103*, 6236.
(22) Ruiz-Gracia, J.; Moreno, A.; Brezesinski, G.; Mohwald, H.; Mas-Oliva, J.; Castillo, R. *J. Phys. Chem. B* **2003**, *107*, 11117.
(23) Tsukanova, V.; Grainger, D. W.; Salesse, C. *Langmuir* **2002**, *18*, 5539.
(24) Wiegart, L.; Struth, B.; Tolan, M.; Terech, P. *Langmuir* **2005**, *21*, 7349.
(25) Polverini, E.; Arisi, S.; Cavatorta, P.; Berzina, T.; Cristofolini, L.; Fasano, A.; Riccio, P.; Fontana, M. P. *Langmuir* **2003**, *19*, 872.
(26) Korl, S.; Ross, M.; Sieber, M.; Kunneke, S.; Galla, H. J.; Janshoff, A. *Biophysical J.* **2000**, *79*, 904.
(27) Ihalainen, P.; Peltonen, J. *Langmuir* **2003**, *19*, 2226.
(28) Yu, Z.; Jin, J.; Cao, Y. *Langmuir* **2002**, *18*, 4530.
(29) Dumas, F.; Lebrun, C. M.; Tocanne, J. *FEBS Lett.* **1999**, *458*, 271.
(30) Killan, A. *Biochim. Biophys. Acta* **1998**, *1376*, 401.
(31) Bloom, M. E.; Mouritsen, O. G. *Q. Rev. Biophys.* **1991**, *24*, 293.
(32) Mouritsen, O. G.; Biltonen, R. L. In *Protein−Lipid Interactions;* Watts, A., Ed.; Elsevier: Amsterdam, The Netherlands, 1993; p 1−39.
(33) Dubreil, L.; Vie, V.; Beaufils, S.; Marion, D.; Renault, A. *Biophys. J.* **2003**, *85*, 2650.
(34) Narsimhan, G.; Uraizee, F. *Biotechnol. Prog.* **1992**, *8*, 187.
(35) McManus, J. J.; Radler, J. O.; Dawson, K. A. *J. Phys. Chem. B* **2003**, *107*, 9869.
(36) Prausnitz, J. M. *Pure Appl. Chem.* **2003**, *75*, 859.
(37) Onda, M.; Hirose, M. *J. Biol. Chem.* **2003**, *278*, 23600.
(38) Ladokhin, A. S. In *Encyclopedia of Analytical Chemistry*; Meyers, R. A., Ed.; John Wiley & Sons. Ltd.: Chichester, U.K. 2000; 5768.
(39) Grossman, N.; Ilovitz, E.; Chaims, O.; Salman, A.; Jagannathan, R.; Mark, S.; Cohen, B.; Gopas, J.; Mordechai, S. Ž. *J. Biochem. Biophys. Methods* **2001**, *50*, 53.
(40) Casals, C.; Miguel, E.; Perez-Gil, J. *Biochem. J.* **1993**, *296*, 585.
(41) Wertz, C. F.; Santore, M. M. *Langmuir* **1999**, *15*, 8884.
(42) Mine, Y. *Trends Food Sci. Technol.* **1995**, *6*, 225.
(43) Shaoyong, Y.; Jinhua, H.; Xiaoyun, P.; Ping, Y.; Ming, J. *Langmuir* **2006**, *22*, 2754.